

Reaction Products with Internal Energy beyond the Kinematic Limit Result from Trajectories Far from the Minimum Energy Path: An Example from $\text{H} + \text{HBr} \rightarrow \text{H}_2 + \text{Br}$

Andrew E. Pomerantz,[‡] Jon P. Camden,[‡] Albert S. Chiou,[‡] Florian Ausfelder,^{‡,†} Navdeep Chawla,[§] William L. Hase,[§] and Richard N. Zare^{*,‡}

Department of Chemistry, Stanford University, Stanford, California 94305-5080, and Department of Chemistry and Biochemistry, Texas Tech University, Lubbock, Texas 79409-1061

Received August 20, 2005; E-mail: zare@stanford.edu

Townsend et al.¹ have recently shown in the photodissociation of formaldehyde to form H_2 and CO that trajectories straying far from the minimum energy path are more common than previously expected. Such mechanisms appear to be operative in other situations.² We demonstrate here that trajectories far from the minimum energy path are, in general, responsible for production of highly internally excited products.

Valentini and co-workers^{3,4} have noticed that many direct, elementary chemical reactions do not significantly populate a large number of energetically accessible quantum states, even though those states often have large statistical weights; they explain this behavior with a simple mechanism in which the nuclei are confined to remain collinear so the trajectory travels near (but not strictly along) the minimum energy path. Under these assumptions, this model shows that not all of the total energy can go into internal modes. Instead, the energy available for internal excitation is constrained to a fraction of the total energy; the magnitude of this constraint depends only on the reaction kinematics (nuclear masses), so the energy available to internal modes is commonly said to be "kinematically constrained." We present experimental evidence that a small but significant fraction of the $\text{H} + \text{HBr}$ reactive trajectories do not obey this kinematic constraint. Moreover, we make a general argument that the usually applicable kinematic limit is broken at high collision energy because some reactive collisions deviate significantly from the minimum energy path.

Figure 1a shows the rotational state distribution for the reaction $\text{H} + \text{HBr} \rightarrow \text{H}_2(\nu' = 2, j') + \text{Br}$ at 53 kcal/mol collision energy. These measurements employ a photoinitiated reaction technique with (2+1) resonance-enhanced multiphoton ionization (REMPI) detection of the reaction products.⁵⁻⁷ For this collision energy and product vibrational level, rotational states $j \leq 18$ are energetically allowed, but only states $j \leq 11$ are kinematically allowed. In good qualitative agreement with the kinematic constraint, 95% of the population falls in the kinematically allowed states, even though these states comprise only 53% of the statistical weight. Nevertheless, measurable population was recorded in all but one energetically allowed rotational state, including six states whose internal energies exceed the kinematic limit.

Quasi-classical trajectory (QCT) calculations were performed to understand why even a small fraction of reactive collisions violate the kinematic limit. The calculations used the VENUS program⁸ to integrate trajectories on a LEPS potential energy surface.⁹ As shown in Figure 1a, nearly quantitative agreement is obtained between the calculations and experiment. This agreement makes

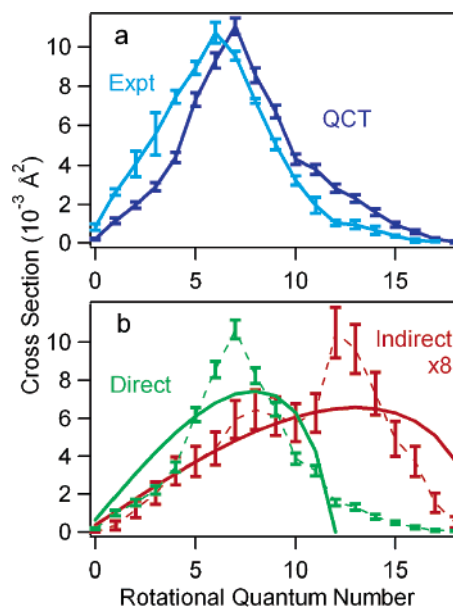


Figure 1. Product rotational distributions for the chemical reaction $\text{H} + \text{HBr} \rightarrow \text{H}_2(\nu' = 2, j') + \text{Br}$ at a collision energy of 53 kcal/mol. Figure 1a shows the measured (light blue) and QCT calculated (dark blue) state distributions; only relative cross-sections are measured, so the experimental result is normalized to match the QCTs. Note that the measured data contain a minor contribution from reaction at a lower collision energy due to a small amount of HBr photolysis producing spin-orbit excited Br. The theoretical distribution shown here is corrected for this effect by calculating distributions at both energies and taking their weighted sum.⁵ This correction is quite small; corrected and uncorrected (not shown) QCT distributions lie within their uncertainties. Figure 1b shows the calculated distributions from the direct and indirect reactive trajectories (green and red dashed lines, respectively). Cross-sections for the indirect mechanism are multiplied by a factor of 8. Figure 1b also shows the (arbitrarily normalized) purely statistical state distributions assuming all of the energy (solid red line) or only the kinematically constrained energy (solid green line) is available for internal excitation.

us believe that the QCT calculations provide a reliable qualitative explanation of the reaction mechanism.

The QCT calculations indicate that two distinct mechanisms operate in this $\text{H}' + \text{HBr} \rightarrow \text{H}'\text{H} + \text{Br}$ reaction; first, a direct reactive mechanism in which H' collides with HBr and forms a $\text{H}'\text{H}$ product that recoils away immediately; second, an indirect reactive mechanism in which H' suffers several collisions with HBr before the $\text{H}'\text{H}$ product is formed. This mechanism is similar to an orbiting resonance proposed by Aker and Valentini.⁹ Indirect reactive trajectories are identified by counting the turning points in the separation between H' and the HBr center of mass. Reactive trajectories with more than one turning point occurring before the product is formed are considered indirect; the $\text{H}'\text{H}$ product of a

[‡] Stanford University.

[§] Texas Tech University.

[†] Present address: Departamento de Química Física I Facultad de Ciencias Químicas, Universidad Complutense, E-28040 Madrid, Spain.

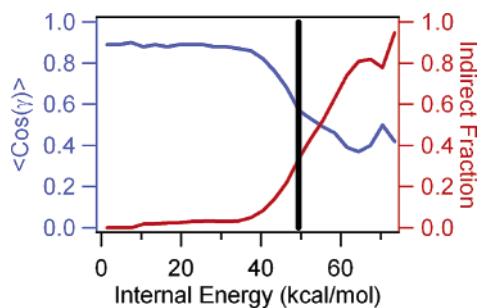


Figure 2. Average value of $\cos(\gamma)$ evaluated at the transition state (blue) and fraction of reactive trajectories that are indirect (red) as a function of the internal energy of the H_2 product. $\cos(\gamma) = 1$ for a collinear transition state and $\cos(\gamma) = 0$ for a bent transition state. The kinematically constrained energy available to internal modes is indicated by the vertical black bar. All reactive trajectories, not just those with $\nu' = 2$, are included in this plot.

particular trajectory is considered to be formed when the $\text{H}'\text{-H}$ separation becomes less than the separation at the outer turning point of the $\text{H}'\text{H}$ vibration for that particular trajectory.

Figure 1b presents calculated rotational distributions for the reaction $\text{H} + \text{HBr} \rightarrow \text{H}_2(\nu' = 2, j') + \text{Br}$ for the two different mechanisms. The total cross-sections and rotational distributions differ substantially; in particular, the total cross-section is considerably larger for the direct reactive mechanism, and the rotational distribution of the indirect reactive mechanism has a stronger preference for populating highly internally excited states. Additionally, the figure shows the purely statistical rotational distributions obtained if all the reaction energy is able to enter internal modes (red) and if only the kinematically constrained energy is available for internal excitation (green); the purely statistical state distribution is proportional to the total degeneracy of each product state, and it is the distribution that would occur in the absence of dynamical constraints.¹⁰ The rotational distribution for the indirect reactive mechanism is qualitatively matched by the statistical distribution obtained if all the energy is allowed to go into internal modes. Similarly, the rotational distribution for the direct reactive mechanism is qualitatively matched by the statistical distribution obtained if only the kinematically constrained energy is available for internal excitation. These results indicate that direct reactive collisions are well described by the kinematic constraint model, whereas the indirect reactive trajectories populate states without any apparent constraint, dynamic or kinematic. This latter result is typical of trajectories proceeding through long-lived complexes, as is the case for these indirect trajectories. It must be emphasized that kinematically constrained and unconstrained statistical state distributions are models, not fits, and they contain no adjustable parameters.

Additional understanding of these trajectories that violate the kinematic limit can be gained by studying the extent to which the trajectories stay near the collinear minimum energy path. To determine the dynamically relevant reaction geometry, the Jacobi angle γ was calculated at the transition state of each trajectory. The Jacobi angle γ is defined as the angle between the internuclear axis in HBr and the line connecting H' with the HBr center of mass;¹¹ the transition state is defined as the coordinates of the trajectory in which potential energy is maximized. The average value of $\cos(\gamma)$ evaluated at the transition state was then calculated as a function of internal energy of the resulting H_2 product; this result is presented in Figure 2. Also presented in Figure 2 is the relative importance of indirect trajectories in populating states of different internal energy.

Two regimes can be clearly distinguished in this figure. H_2 products with low internal excitation are formed almost exclusively

from direct trajectories and are nearly perfectly collinear at the transition state. H_2 products with high internal excitation are formed mainly from indirect trajectories having bent transition states. Additionally, the maximum kinematically allowed internal energy is indicated by the vertical black line on the figure. This kinematic limit cleanly divides the two regimes. Note that whereas the barrier to reaction for a perpendicular $\text{H}'\text{-H-Br}$ approach (29 kcal/mol) is higher than the barrier for a collinear geometry (2 kcal/mol),¹² both barriers can be overcome at the high collision energy (53 kcal/mol) studied here.

With these data as an example, a general argument can be made about the origin of highly internally excited products of chemical reactions. The kinematic limit model shows that the amount of energy available to internal modes is kinematically constrained, under the assumption that reactive collisions are direct and proceed near the minimum energy path, with all nuclei remaining collinear (for atom + pseudo-diatom collisions). This model successfully predicts that many energetically accessible product quantum states will not be populated for chemical reactions in general. This behavior is indeed observed for this system, as 95% of reactive products falls in kinematically allowed states, but measurable population is observed here in many kinematically forbidden states. Trajectories that populate states with internal energies in violation of the kinematic limit must come from collisions that violate the assumptions of that model. These events are rare, but they occur frequently enough to be observable. Reactions at high total energy are not required to stay near the minimum energy path. We propose that reaction products with internal energies exceeding the kinematic constraint arise from trajectories that deviate significantly from the minimum energy path. In the $\text{H} + \text{HBr}$ reaction, these products are formed from indirect reactions whose transition states contain a significant amount of bent character. Although the exact mechanism for trajectories violating the kinematic limit may differ from system to system, we suggest that products of a direct reaction with internal energy exceeding the kinematic limit can, in general, be attributed to reactive collisions straying far from the minimum energy path.

Acknowledgment. The Stanford group was supported by the National Science Foundation Grant 0242103, and the Texas Tech group by the National Science Foundation Grant 0412677 and the Robert A. Welch Foundation Grant D-0005.

Supporting Information Available: Movies of representative trajectories for direct and indirect reactive mechanisms. This material is available free of charge via the Internet at <http://pubs.acs.org>.

References

- (1) Townsend, D.; Lahankar, S. A.; Lee, S. K.; Chambreau, S. D.; Suits, A. G.; Zhang, X.; Rheinecker, J.; Harding, L. B.; Bowman, J. M. *Science* **2004**, *306*, 1158–1161.
- (2) Sun, L.; Song, K.; Hase, W. L. *Science* **2002**, *296*, 875–878.
- (3) Picconatto, C. A.; Srivastava, A.; Valentini, J. J. *J. Chem. Phys.* **2001**, *114*, 1663–1671.
- (4) Valentini, J. J. *J. Phys. Chem. A* **2002**, *106*, 5745–5759.
- (5) Pomerantz, A. E.; Ausfelder, F.; Zare, R. N.; Althorpe, S. C.; Aoiz, F. J.; Bañares, L.; Castillo, J. F. *J. Chem. Phys.* **2004**, *120*, 3244–3254.
- (6) Ausfelder, F.; Pomerantz, A. E.; Zare, R. N.; Althorpe, S. C.; Aoiz, F. J.; Bañares, L.; Castillo, J. F. *J. Chem. Phys.* **2004**, *120*, 3255–3264.
- (7) Pomerantz, A. E.; Ausfelder, F.; Zare, R. N.; Huo, W. M. *Can. J. Chem.* **2004**, *82*, 723–729.
- (8) Hase, W. L. et al. *VENUS96: A General Chemical Dynamics Program*, Quantum Chemistry Program Exchange: Detroit, Michigan, 1996.
- (9) Aker, P. M.; Valentini, J. J. *Isr. J. Chem.* **1990**, *30*, 157–178.
- (10) Kinsey, J. L. *J. Chem. Phys.* **1971**, *54*, 1206–1217.
- (11) Levine, R. D.; Bernstein, R. B. *Molecular Reaction Dynamics and Chemical Reactivity*; Oxford University Press: New York, 1987.
- (12) This barrier is calculated for the LEPS surface and is in good qualitative agreement with a more accurate surface; see: Lynch, G. C.; Truhlar, D. G.; Brown, F. B.; Zhao, J. *J. Phys. Chem.* **1995**, *99*, 207–225.

JA055440A